

- Chatterjee, *Glycobiology* **5**, 117 (1995).
16. G. Y. Ishioka *et al.*, *J. Immunol.* **148**, 2446 (1992).
  17. C. V. Harding, J. Kihlberg, M. Elofsson, G. Magnusson, E. R. Unanue, *ibid.* **151**, 2419 (1993).
  18. J. S. Haurum *et al.*, *J. Exp. Med.* **180**, 739 (1994).
  19. E. Michaelsson *et al.*, *ibid.*, p. 745.
  20. S. Xu *et al.*, *J. Immunol.* **153**, 2568 (1994).
  21. S. Porcelli and M. B. Brenner, unpublished observations.
  22. P. A. Sieling *et al.*, in preparation.
  23. E. L. Reinherz, P. C. Kung, G. Goldstein, R. H. Levey, S. F. Schlossman, *Proc. Natl. Acad. Sci. U.S.A.* **77**, 1588 (1980).
  24. E. J. Favaloro *et al.*, *Disease Markers* **4**, 261 (1986).
  25. L. H. Martin, F. Calabi, F.-A. Lefebvre, C. A. G. Bilsland, C. Milstein, *Proc. Natl. Acad. Sci. U.S.A.* **84**, 9189 (1987).
  26. F. M. Brodsky and P. Parham, *J. Immunol.* **128**, 129 (1982).
  27. L. Shiue, S. D. Gorman, J. R. Parnes, *J. Exp. Med.* **168**, 1993 (1988).
  28. S. Porcelli, M. B. Brenner, H. Band, *Immunol. Rev.* **120**, 137 (1991).
  29. S. W. Hunter and P. J. Brennan, *J. Biol. Chem.* **265**, 9272 (1990).
  30. DN T cell lines were derived from peripheral blood (BDN2) or a tuberculoid leprosy lesion (LDN4) by immunomagnetic depletion of CD4, CD8, and  $\gamma\delta$  T cells and culture with *M. leprae* in the presence of PBMCs treated with granulocyte-macrophage colony-stimulating factor (200 U/ml) and IL-4 (100 U/ml) (to induce CD1 expression) (2). The following antibodies were used for flow cytometry and blocking experiments: OKT6, CD1a (23); WM-25, CD1b (24); 10C3, CD1c (25); W6/32 HLA-A, B, and C (26); DK22, HLA-DR (Dako, Carpinteria, CA); OKT4, CD4 (23); OKT8, CD8 $\alpha$  (23); 2ST8-5H7, CD8 $\beta$  (27); WT31, TCRA $\beta$ , (Becton-Dickinson, San Jose, CA); and TCR $\gamma\delta$  (28).
  31. Target cells were derived from granulocyte-macrophage colony-stimulating factor- and IL-4-treated PBMCs. Nonadherent cells were discarded, and adherent cells (CD1-positive) were removed with phosphate-buffered saline (PBS) containing 5 mM EDTA (10 min). Target cells ( $1 \times 10^6$  cells per milliliter) were incubated with media, *M. leprae* (2  $\mu$ g/ml), or *M. leprae* LAM (2  $\mu$ g/ml) for 16 hours, washed, then labeled with  $^{51}\text{Cr}$ . Antibodies to CD1 (5  $\mu$ g/ml) were added to target cells (4000 cells per 100  $\mu$ l) and LDN4 T cells for a 5-hour incubation period. Supernatants (75  $\mu$ l) were harvested and counted in a gamma counter.
  32. GPIs were isolated from *M. leprae* by extraction with 50% ethanol and partitioning between phenol and water (29). LAM, LM, and PIMs were separated by gel filtration chromatography on Sephacryl S-200 and analyzed (2  $\mu$ g each) by SDS-PAGE (15% acrylamide) with silver staining (12).
  33. To improve solubility, we treated both LM and  $\alpha$ -mannosidase-treated LM with 0.1 N NaOH for 4 hours at 37°C. The fatty acids were removed by extraction with  $\text{CHCl}_3:\text{CH}_3\text{OH}$  as described (29). The aqueous layers were desalted with Bio-Gel P-2 column chromatography (1 cm by 100 cm; total volume, 90 ml), and 1-ml fractions were collected. The elution position of the salt was measured by conductivity (fractions 70 to 78). The voided fractions (fractions 23 to 28) were pooled, dried, and exchanged with  $\text{D}_2\text{O}$ .
  34. For the mannosidase treatment of LM, we solubilized 500  $\mu$ g of LM in 50 mM ammonium acetate buffer, pH 4.5, and digested it with 2.5 U of  $\alpha$ -D-mannosidase (20  $\mu$ l) from jack bean meal (V-LABS, Covington, LA) for 16 hours at 37°C. The enzyme was denatured by boiling for 2 min and centrifuged to remove insoluble material.
  35. For the protease treatment of LAM, proteinase K (0.2  $\mu$ g) (Boehringer Mannheim, Indianapolis, IN) was added to 250  $\mu$ g of *M. leprae* LAM in ammonium bicarbonate buffer, and the solution was incubated at 55°C for 1 hour. The mixture was boiled for 2 min to inactivate the enzyme, and the sample was lyophilized.
  36. J. Woo, C. Shinohara, K. Sakai, K. Hasumi, A. Endo, *Eur. J. Biochem.* **207**, 383 (1995).
  37. Supported by grants from NIH (B.R.B., AI 07118;

P.J.B., AI 18357; M.B.B., AI 28973; M.K., CA 52511; R.J.M., CA 09173; R.L.M., AI 22553, AI 36069, and AR 40312; T.I.P., CA 09120; S.A.P., AR 01854; P.A.S., CA 09120), the Howard Hughes Medical Institute (B.R.B.), the Arthritis Foundation (S.A.P., Investigator Award), the UNDP-World Bank-World Health Organization Special Programme for Research and Training in Tropical Diseases (IMMLEP) (R.L.M.), the Dermatologic Research

Foundation of California (R.L.M.), the Heiser Trust (P.A.S.), and NIH contract AI 05074 to Colorado State University. We thank T. Rea for helpful discussions and X. Wang for TCR analysis. The *L. major* LPG was a gift from S. Turco, University of Kentucky; the *S. pyogenes* LTA was a gift from I. van de Rijn, Wake Forest University.

6 April 1995; accepted 30 May 1995

## Targeted Disruption of Mouse EGF Receptor: Effect of Genetic Background on Mutant Phenotype

David W. Threadgill, Andrzej A. Dlugosz, Laura A. Hansen, Tamar Tennenbaum, Ulrike Lichti, Della Yee, Christian LaMantia, Tracy Mourton, Karl Herrup, Raymond C. Harris, John A. Barnard, Stuart H. Yuspa, Robert J. Coffey, Terry Magnuson\*

Gene targeting was used to create a null allele at the epidermal growth factor receptor locus (*Egfr*). The phenotype was dependent on genetic background. EGFR deficiency on a CF-1 background resulted in peri-implantation death due to degeneration of the inner cell mass. On a 129/Sv background, homozygous mutants died at mid-gestation due to placental defects; on a CD-1 background, the mutants lived for up to 3 weeks and showed abnormalities in skin, kidney, brain, liver, and gastrointestinal tract. The multiple abnormalities associated with EGFR deficiency indicate that the receptor is involved in a wide range of cellular activities.

The expression pattern and functional analysis of EGFR and its ligands suggest that EGFR is important for embryo development, tissue differentiation, and cellular function (1, 2). The only known genetic alteration is a point mutation (*Egfr<sup>wa2</sup>*) in the kinase domain that leads to diminished receptor activity (3). The phenotype of waved hair and sporadic open eyelids is similar to that of mice deficient for transforming growth factor- $\alpha$  (*Tgfa<sup>wa1</sup>*) (4).

A null allele (*Egfr<sup>m1Cwr</sup>*) at the *Egfr* locus was created by homologous recombination in 129/Sv-derived D3 embryonic stem cells (Fig. 1A). Seven independently targeted lines were identified (5). Germline chimeric males were mated to 129/Sv females to establish a co-isogenic strain carrying the

*Egfr<sup>m1Cwr</sup>* allele. The allele was then bred into the closed-colony, random-bred CF-1 and CD-1 lines. When homozygous, the mutation resulted in peri-implantation lethality in CF-1 mice, mid-gestation lethality in 129/Sv mice, and perinatal lethality in CD-1 mice. All three phenotypes were fully penetrant and nonoverlapping. Aberrant splicing around the targeted exon was detected joining exon 1 to either exon 3 or exon 5 (Fig. 1B). The former splicing event would create a nonsense protein, whereas the latter retains the reading frame and removes domain 1 of the extracellular region. Although a truncated mRNA is produced, *Egfr<sup>m1Cwr</sup>* homozygous pups showed no evidence of an altered EGFR (Fig. 1C) and no indication of EGF-inducible tyrosine phosphorylation.

On a CF-1 background, *Egfr<sup>m1Cwr</sup>* homozygous embryos died before embryonic day 7.5 (E7.5) (Table 1). The three mutant embryos recovered at E6.5 consisted of a small mass of unorganized cells. Morphologically normal embryos were observed in 51 implantation sites from *Egfr<sup>m1Cwr</sup>/+*  $\times$  *+/+* control crosses, suggesting that the empty decidua from *Egfr<sup>m1Cwr</sup>/+*  $\times$  *Egfr<sup>m1Cwr</sup>/+* heterozygous crosses were derived from *Egfr<sup>m1Cwr</sup>* homozygous embryos. Preimplantation development proceeded normally, and after transfer of blastocysts to serum-supplemented medium, *Egfr<sup>m1Cwr</sup>* homozy-

D. W. Threadgill, D. Yee, C. LaMantia, T. Mourton, T. Magnuson, Department of Genetics, Case Western Reserve University, 10900 Euclid Avenue, Cleveland, OH 44106-4955, USA.

A. A. Dlugosz, L. A. Hansen, T. Tennenbaum, U. Lichti, S. H. Yuspa, Laboratory of Cellular Carcinogenesis and Tumor Promotion, National Cancer Institute, National Institutes of Health, Bethesda, MD 20892, USA.

K. Herrup, Alzheimer Research Laboratory, Department of Neurology, Case Western Reserve University, Cleveland, OH 44106, USA.

R. C. Harris, Department of Medicine, Vanderbilt University, Nashville, TN 37232, USA.

J. A. Barnard, Department of Pediatrics, Vanderbilt University, Nashville, TN 37232, USA.

R. J. Coffey, Departments of Medicine and Cell Biology, Vanderbilt University, Nashville, TN 37232, USA.

\*To whom correspondence should be addressed.

**Fig. 1.** Targeted disruption and expression analysis of *Egfr*. **(A)** Strategy for targeting *Egfr* (14). Targeting resulted in replacement of 155 base pairs (bp) surrounding the splice acceptor site of exon 2 with a Neo cassette and insertion of a new Apa I site shortening the wild-type 15-kb fragment to 11 kb. Exons are numbered. A, Apa I. **(B)** RT-PCR products from *Egfr* transcripts in total liver RNA from wild-type (+/+), *Egfr<sup>m1Cwr</sup>* heterozygous (+/-) and homozygous (-/-) animals. RNA was reverse-transcribed with random hexamers. PCR primers: Exon 1, GGGGCGTTG-GAGGAAAAGAA; and exon 7, ATGAGTGGT-GGGCAGGTG. Sizes of PCR products are indicated on the left (in kilobases) and exon splice junctions on the right. **(C)** Protein immunoblot analysis of liver-detergent lysates. Mice were injected with phosphate-buffered saline (P) or EGF (E) for autophosphorylation (15). The blot was consecutively probed with antibody to EGFR (anti-EGFR) (Life Technologies), anti-phosphotyrosine (ICN), and anti-ErbB2 (Transduction Laboratories) as described (3). Antibody binding was detected by enhanced chemiluminescence (Amersham). Molecular sizes are indicated on the left (in kilodaltons) and immunoreactive proteins detected on the right.

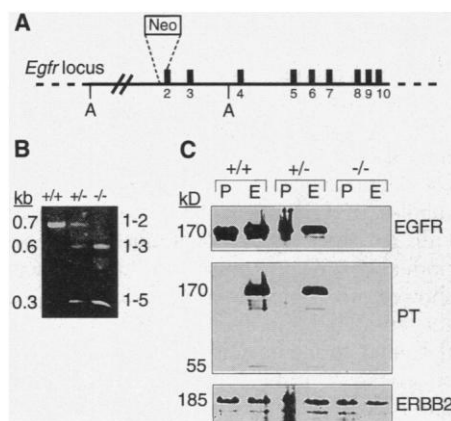


**Table 1.** Genetic background and lethality of *Egfr<sup>m1Cwr</sup>* heterozygous crosses. On a CD-1 background, 6% of fetuses were dead at E18.5, all of which genotyped as -/- . n, number of pups or embryos examined; A, empty decidua; P, postnatal day; E, embryonic day.

Day	n	+/+ (%)	+/- (%)	-/- (%)	A (%)
<i>CF-1</i>					
P0	56	38	63	0	
E7.5-8.5	36	25	61	0	14
E6.5	117	23	49	2	26
E3.5	150	20	53	27	
<i>129/Sv</i>					
P0	41	34	66	0	
E12.5-13.5	13	15	54	23*	8
<i>CD-1</i>					
P0	238	30	54	16	
E18.5	81	24	50	20	
E15.5-17.5	73	22	56	22	
E12.5-13.5	45	29	47	20	4

\*All embryos dissected at this time were resorbing.

gous embryos hatched from their zona pellucida and attached to culture plates. However, after 5 days in culture, *Egfr<sup>m1Cwr</sup>* homozygous embryos did not grow, although normal littermates produced extended embryonic outgrowths (5).

Analysis of E4.5-4.8 implantation sites showed that 6 out of 32 embryos from heterozygous crosses had small, loosely arranged inner cell masses (ICMs) with no distinct endoderm (Fig. 2, A and B). This phenotype was observed in only 2 out of 40 embryos from control crosses, suggesting that the abnormal embryos were *Egfr<sup>m1Cwr</sup>* homozygous mutants. By E5.1-5.5, when normal embryos had differentiated ectoplacental cone and extraembryonic ectoderm, 13 out of 61 embryos from heterozygous crosses were collapsed, with no embryonic

tissue organization (5). At E6.5, 8 out of 31 implantation chambers lacked an embryo and had filled with maternal blood (Fig. 2, C and D). The decidualization reaction of the maternal stromal cells progressed normally, and H19-positive primary trophoblast giant cells were detected around the empty implantation sites (Fig. 2, C and D) (6). From control crosses, only 2 of 98 decidua lacked an embryo at E5.1 to 6.5. Thus, contrary to previous hypotheses (2, 7), the ICM, and not the trophoctoderm (TE), requires EGFR in CF-1 embryos for survival.

Analysis of *Egfr<sup>m1Cwr</sup>* homozygosity on an inbred 129/Sv genetic background revealed a second distinct phenotype. At E12.5-13.5, 23% of decidua contained extraembryonic membranes with resorbing *Egfr<sup>m1Cwr</sup>* homozygous embryos and placentas smaller than those of wild-type littermates (22.1 + 1.7 mg wet weight versus 46.8 + 2.8 mg). The spongiotrophoblast layer was greatly reduced and the labyrinthine trophoblast was disorganized with a reduced cell number (Fig. 2, E and F). The organization and cell number of the trophoblast giant-cell layer was unaffected. These data indicate that homozygosity for *Egfr<sup>m1Cwr</sup>* produces a mid-gestation lethality in 129/Sv embryos due to a placental defect.

On a CD-1 genetic background, *Egfr<sup>m1Cwr</sup>* homozygous embryos demonstrated a perinatal lethality (Table 1). Although birthweight was normal, *Egfr<sup>m1Cwr</sup>* homozygous pups showed reduced growth and progressive wasting. When most normal littermates were removed, some *Egfr<sup>m1Cwr</sup>* homozygous pups survived as long as postnatal day 18 (P18), but they were only 30 to 35% the weight of normal littermates. Newborn *Egfr<sup>m1Cwr</sup>* homozygous pups were distinguished by open eyes and rudimentary

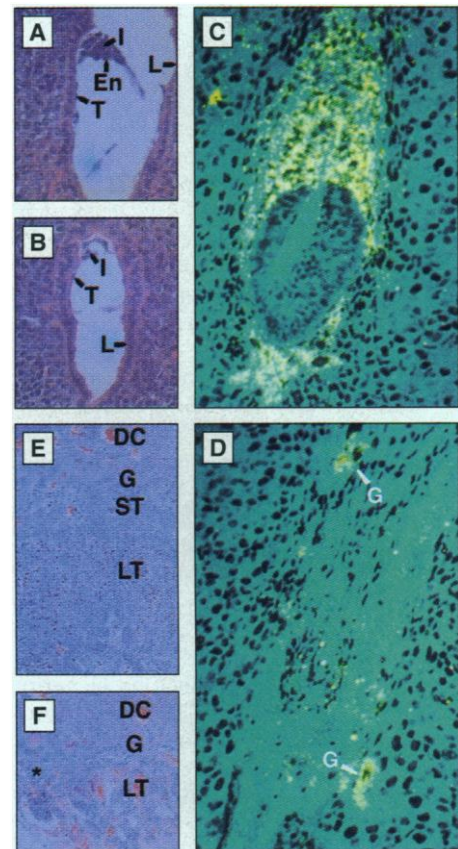


**Fig. 2.** Histological and in situ analysis of peri-implantation embryos and mid-gestation placentas (16). **(A to D)** Uterine sections from CF-1 heterozygous crosses at (A and B) E4.5-4.8 (magnification,  $\times 400$ ; staining with H&E) and (C and D) E6.5 ( $\times 200$ ; confocal images of H19 mRNA in situ). (A) and (C) are normal and (B) and (D) are abnormal decidua. **(E and F)** H&E-stained sections of E13.5 placentas from 129/Sv (E) wild-type and (F) *Egfr<sup>m1Cwr</sup>* homozygous embryos ( $\times 40$ ). I, inner cell mass; T, trophoctoderm; L, luminal epithelium; DC, decidua; ST, spongiotrophoblast; LT, labyrinthine trophoblast. Asterisk, residual ST.

waved whiskers that uniformly curled anteriorly and were fragile. Scanning electron microscopy from E14.5-18.5 showed that the eyelids failed to form (5).

Although the developing hair follicles of *Egfr<sup>m1Cwr</sup>* homozygous mice appeared normal at birth, by P5 they were disoriented and irregularly placed (Fig 3, A and B). The hair shaft showed premature separation from the inner root sheath. Hair keratinization and maturation of the inner root sheath was also premature. These maturation defects predict that fragility is responsible for the delayed, fuzzy appearance of emerging hair. The epidermis of *Egfr<sup>m1Cwr</sup>* homozygous mice appeared otherwise normal until thinning at P18 (5).

Hair follicles in *Egfr<sup>m1Cwr</sup>* homozygous skin expressed keratin 6 prematurely and ectopically in the region just above the hair bulb, and  $\alpha 3\beta 1$  and  $\alpha 6\beta 4$  integrins were

expressed ectopically along the outer root sheath of follicles growing deep in the dermis (Fig. 3, C and D) (5). Laminin I, collagen IV, keratins 1, 10, and 14, loricrin, filaggrin, and fibronectin distribution were unaffected by the EGFR mutation (5). An increase in suprabasal expression of  $\alpha 3\beta 1$  integrin in the epidermis was detected in *Egfr<sup>m1Cwr</sup>* homozygous mice as early as P2 (5). Because EGFR ligands have been shown to influence integrin expression and keratinocyte migration in vitro (8), aberrant expression of  $\alpha 3\beta 1$  or  $\alpha 6\beta 4$  could explain the abnormal follicle placement.

Although interfollicular epidermal proliferation, as monitored by 5-bromodeoxyuridine (BrdU) incorporation, was similar to that of controls at birth, by P2 and thereafter it declined, attaining only 32% of the wild-type labeling index at P8 (5). BrdU labeling in the infundibulum and bulb of the hair follicles was unaffected. Cultured *Egfr<sup>m1Cwr</sup>* homozygous keratinocytes that did not respond to TGF- $\alpha$  were responsive to growth stimulation by keratinocyte, acidic fibroblast, and basic fibroblast growth factors (all at 10 ng/ml) (5). Thus, EGFR may regulate proliferation of the epidermis (9) and orientation and maturation of hair follicles.

The epithelial lining of *Egfr<sup>m1Cwr</sup>* homozygous tongues showed reduced numbers of fungiform papillae (Fig. 3, E and F); those present at P12 were disorganized with no obvious taste buds. The filiform papillae were also abnormal, with sparse connective tissue, and the tongues contained less than normal amounts of interspersed adipose tissue.

The *Egfr<sup>m1Cwr</sup>* homozygous gastrointestinal tract showed minor alterations. Although the squamous epithelium of the esophagus was relatively normal, BrdU labeling was markedly decreased in the basal layer in both P12 and P18 *Egfr<sup>m1Cwr</sup>* homozygotes (5). The number and spatial orientation of H<sup>+</sup>/K<sup>+</sup>-adenosine triphosphatase (ATPase)-positive parietal cells and PAS-staining surface mucous cells were normal in the glandular portion of the stomach (5). The small intestinal crypt-villus architecture was preserved and absorptive epithelial, goblet, and Paneth cell lineages were present. Lactase-phlorizin hydrolase activity was normal in the small intestine (5). The morphology of the colon was normal through P12, but the colonic epithelium of P18 *Egfr<sup>m1Cwr</sup>* homozygous mice had distorted glandular architecture (Fig. 3, G and H). Tall disorganized, branching crypt columns were observed, occasionally in close proximity to short rudimentary crypt columns (Fig. 3, G and H, top insets); BrdU labeling (Fig. 3, G and H, bottom insets) showed a proliferative population of progenitor colonocytes remaining at P18. Although livers were normal at

E17.5, by P8 they had thickened hepatocyte cords, distorted sinusoidal anatomy, and abnormally vacuolized nuclei (5). Hematopoietic cells within sinusoids were normal.

Kidney cell proliferation and nephron morphology were normal. *Lotus tetragonolobus* lectin staining, specific for proximal tubules, and Tamm Horsfall staining, specific for thick ascending limbs, were also normal (5, 10). In contrast, collecting ducts showed progressive cystic dilation in which the epithelial lining of these tubules was flattened, losing its normal cuboidal appearance (Fig. 3, I and J). The dilated tubules did, however, demonstrate normal *Dolichos biflorus* lectin staining (Fig. 3, I and J, insets) (10). Renal malfunction was indicated by elevated blood urea nitrogen after birth (75 mg/dl in P12 *Egfr<sup>m1Cwr</sup>* homozygous mice, 26 mg/dl in normal littermates), increasing to 288 mg/dl at P18 as did serum creatinine (2.4 mg/dl in mutant, 0.1 mg/dl in normal littermates). Thus, EGFR is unnecessary for induction of the metanephric blastema, but is required for differentiation of structures

derived from the ureteric bud.

At E18.5, the overall size of the brain of *Egfr<sup>m1Cwr</sup>* homozygous fetuses was reduced. Cortical regions were most affected; the cerebellar plate, for example, had variably fewer Purkinje cells, a condition persisting postnatally, leading to a reduction in cerebellar size and, concomitantly, a retarded migration of the external granule cell layer (5). All of the various germinative regions were, however, present at the correct time and place.

Cellular migration was defective in several regions, particularly in the cerebral cortex. Although the overall structure of the E18.5 cerebral cortex was comparable to that of wild type (Fig. 4, A and B), the migration of neuroblasts and formation of the *Egfr<sup>m1Cwr</sup>* homozygous cerebral cortical plate was compromised. The ventricular zone was abnormally thick, and the intermediate zone was variable in thickness, with substantial thinning in some *Egfr<sup>m1Cwr</sup>* homozygotes. This suggests that cellular migration may have been slowed or blocked. A similar defect in

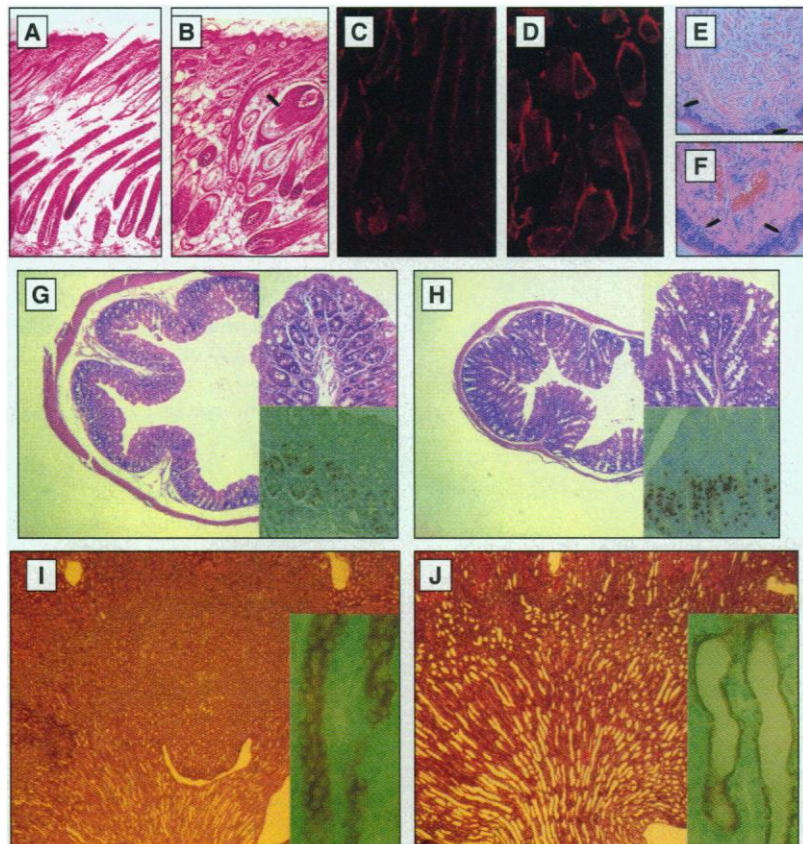


**Fig. 3.** Altered histology, cell proliferation, and marker expression in CD-1 mice. (**A, C, E, G, I**) Wild-type and (**B, D, F, H, J**) *Egfr<sup>m1Cwr</sup>* homozygotes. Dorsal skin sections at (A and B) P12 ( $\times 125$ ) and (C and D) P8 ( $\times 200$ ). (A, B, E, F, I, J) are stained with H&E. Arrow points to an inverted hair follicle. (C and D) Immunohistochemistry with anti- $\alpha 6$  integrin as described (17). (E and F) Tongue sections ( $\times 100$ ). Arrows point to (E) mature taste buds and (F) rudimentary fungiform papillae. (G and H) Cross sections of P18 colons ( $\times 50$ ). Insets show H&E-stained mucosa (top,  $\times 125$ ) and BrdU immunostaining (bottom,  $\times 160$ ). (I and J) Histological appearance of P18 kidneys ( $\times 62.5$ ). Staining with *Dolichos biflorus* lectin (insets,  $\times 500$ ).

cell migration was suggested by the appearance of the anterior regions of the lateral ventricles from which cells migrate into the olfactory bulb and become granule cells. Neurogenesis in this subependymal zone appeared normal although the germinative zones were thickened.

The effect of EGFR on nerve cell survival was particularly marked in the anterior areas of the cerebral cortex at P18 (Fig. 4, C and D). At this stage, *Egfr<sup>m1Cwr</sup>* homozygotes showed atrophy of the entire anterior cerebral cortex, which was reduced to a thin, membrane-like sheet of cells. There was no apparent hydrocephalus. The normal rotation of the hippocampal formation was apparent although the region was abnormally small. More caudal diencephalic structures appeared less disturbed. Other areas of the brain showed cell type-specific defects. In the olfactory bulb, the *Egfr<sup>m1Cwr</sup>* homozygous mice lost nearly all of their mitral and tufted cells by the end of the second postnatal week (Fig. 4, E and F). Whereas glomerular structures in P18 olfactory bulbs appeared normal, the molecular layer of *Egfr<sup>m1Cwr</sup>* homozygous mice was shortened or altogether missing. The absence of neurons was not caused by a failure of neurogenesis, because E18.5 olfactory bulbs were normal in size and cellular constitution (Fig. 4, E and F, insets).

Lungs of *Egfr<sup>m1Cwr</sup>* homozygous mice were similar in morphology to those of normal littermates at E18.5 (5). No differ-

ences were detected in staining of surfactant protein SP-B or the precursors proSP-B and proSP-C. Two out of eight *Egfr<sup>m1Cwr</sup>* homozygotes showed slightly immature lung histology and weaker surfactant staining, which may just reflect their overall 15% growth retardation (11). Other organ systems with no gross histological differences between *Egfr<sup>m1Cwr</sup>* homozygous and wild-type littermates included the pancreas, heart, skeletal muscle, skeleton, teeth, spermatogenesis to P8, and oogenesis to P12.

There are several possible explanations of the genetic background effect on *Egfr<sup>m1Cwr</sup>* homozygous phenotype. Although zygotic transcription does not begin until the eight-cell stage, maternal *Egfr* transcripts and protein are present during preimplantation development (12). As a consequence, any requirement for EGFR by *Egfr<sup>m1Cwr</sup>* homozygous pre- and peri-implantation embryos would have to be supplied by the oocyte pool of protein or transcript. One explanation for survival past implantation is that CD-1 and 129/Sv *Egfr* alleles provide more oocyte-derived EGFR than does a CF-1 allele. To test for a maternal effect, blastocysts from CD-1 *Egfr<sup>m1Cwr</sup>* heterozygous crosses were delayed from implanting for 4 days (13). Such blastocysts undergo a decrease in EGFR levels and *Egfr* expression (13), thus depleting the maternally derived pool of EGFR. When delayed CD-1 embryos were

reactivated, morphologically normal midgestation *Egfr<sup>m1Cwr</sup>* homozygous embryos were recovered at expected frequencies. Semi-quantitative reverse transcriptase-polymerase chain reaction (RT-PCR) with RNA from ovulated eggs also showed no detectable differences between strains in the maternal pool of *Egfr* transcripts. These data argue against differences in oocyte-derived pools of EGFR to explain the peri-implantation lethality.

Genetic differences in maternal uterine environment may also influence the *Egfr<sup>m1Cwr</sup>* homozygous phenotype. Therefore, embryos of one genetic background were reciprocally transferred into uteri of another background at E0.5 and allowed to develop until E13.5 or birth, at which time the three phenotypes can be distinguished. In all cases, the observed phenotypes were embryo- and not uterine-specific, implying that distinct zygotic-modifying genes are involved.

The results presented here for the *Egfr<sup>m1Cwr</sup>* null mutation have important implications for previous work on EGFR, almost all of which has been performed on undefined genetic backgrounds. Our results indicate that EGFR functions in a wide range of cellular and tissue activities that can be modified by genetic background. The mechanism by which these modifications occur will be understood only by identifying strain-specific modifiers.

## REFERENCES AND NOTES

1. E. D. Adamson, *Mol. Reprod. Dev.* **27**, 16 (1990); A. Dardik, R. M. Smith, R. M. Schultz, *Dev. Biol.* **154**, 396 (1992); J. A. Barnard, R. D. Beauchamp, W. E. Russell, R. N. DuBois, R. J. Coffey, *Gastroenterology* **108**, 564 (1995); W. C. Weinberg, P. D. Brown, W. G. Stetler-Stevenson, S. H. Yuspa, *Differentiation* **45**, 168 (1990).
2. S. A. Wood, P. L. Kaye, *J. Reprod. Fertil.* **85**, 575 (1989).
3. N. C. Luetetteke *et al.*, *Genes Dev.* **8**, 399 (1994); K. J. Fowler *et al.*, *Proc. Natl. Acad. Sci. U.S.A.* **92**, 1465 (1995).
4. N. C. Luetetteke *et al.*, *Cell* **73**, 263 (1993); G. B. Mann *et al.*, *ibid.*, p. 249.
5. D. W. Threadgill *et al.*, data not shown.
6. F. Poirier *et al.*, *Development* **113**, 1105 (1991).
7. E. C. Brice, J. X. Wu, R. Muraro, E. D. Adamson, L. M. Wiley, *Dev. Genet.* **14**, 174 (1993).
8. T. E. Carey *et al.*, *Monogr. Natl. Cancer Inst.* **XX**, 75 (1992); J. D. Chen *et al.*, *Exp. Cell Res.* **209**, 216 (1993).
9. A. B. Glick *et al.*, *Proc. Natl. Acad. Sci. U.S.A.* **90**, 6076 (1993); D. R. Roop, H. Huitfeldt, A. Kilkenny, S. H. Yuspa, *Differentiation* **35**, 143 (1987).
10. E. D. Avner and W. E. Sweeney, *Pediatr. Nephrol.* **4**, 372 (1990).
11. A. A. W. Ten Have-Opbroeck, J. A. Dubbeldam, C. J. M. Otto-Verberne, *Anat. Rec.* **221**, 846 (1988).
12. L. M. Wiley, J. X. Wu, I. Harari, E. D. Adamson, *Dev. Biol.* **149**, 247 (1992); B. C. Paria and S. K. Dey, *Proc. Natl. Acad. Sci. U.S.A.* **87**, 4756 (1990).
13. B. C. Paria, S. K. Das, G. K. Andrews, S. K. Dey, *Proc. Natl. Acad. Sci. U.S.A.* **90**, 55 (1993).
14. The pEgfr-T2 targeting vector was constructed from C3H/101 genomic clones. PCR screening for targeted lines was done with primers Egfr-a (5'-CATTAT-TACGGTCTCTCTTTC-3'), residing outside of pEgfr-T2, and Egfr-d (5'-GATCTGAAGTTCCTAT-TCCGAAGTTC-3'), residing inside pEgfr-T2, which

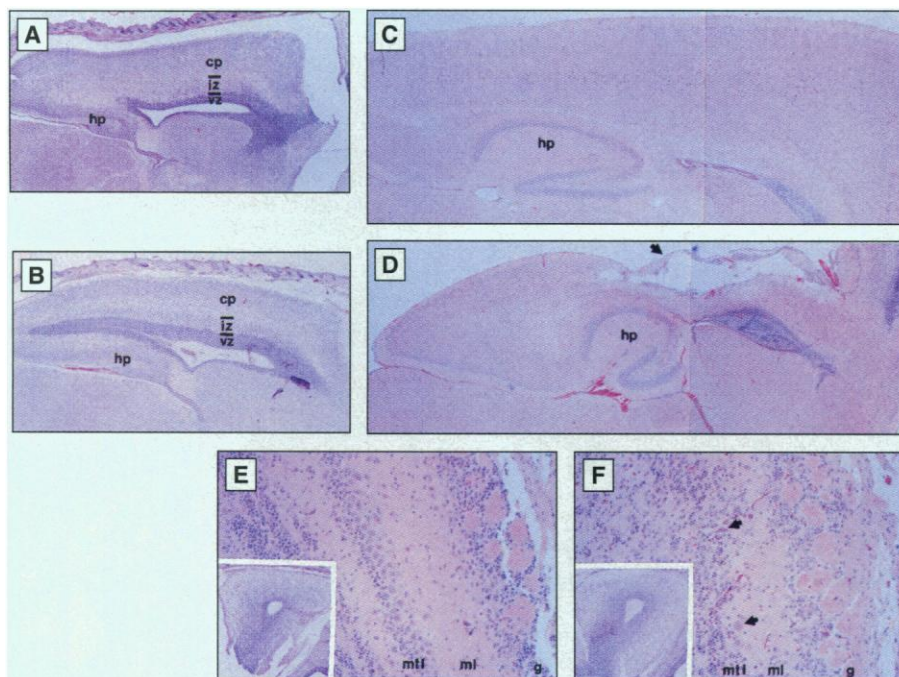


**Fig. 4.** Brain cytoarchitectonics. Parasagittal sections of wild-type (A, C, E) and *Egfr<sup>m1Cwr</sup>* homozygous mice (B, D, F) stained with H&E. (A and B) Cerebral cortex at E18.5 ( $\times 40$ ). (C and D) Cerebral cortex at P18 ( $\times 40$ ). Arrow in (D) points to atrophied cerebral cortex. (E and F) Structure of olfactory bulb at P18 ( $\times 200$ ) and at E18.5 (insets,  $\times 40$ ). Arrows in (F) point to remaining mitral cells. cp, cortical plate; g, glomerular layer; hp, hippocampal formation; iz, intermediate zone; ml, molecular layer; mtl, mitral cells; vz, ventricular zone.

amplify a 1.2-kb fragment. The probe used for Southern (DNA) blot hybridizations to verify targeted lines is a 2.1-kb Eco RI fragment from intron 1 located upstream of the sequences used in the construction of pEgfr-T2. The targeting frequency was 1/125.

15. R. W. Donaldson and C. W. Cohen, *Proc. Natl. Acad. Sci. U.S.A.* **89**, 8477 (1992).
16. Pieces of whole uteri containing implantation sites, placentas, and brains were fixed in 4% paraformaldehyde, embedded in paraffin, and 7- $\mu$ m sections collected on glass slides before staining with hematoxylin-eosin (H&E) [R. Zeller, in *Cur. Prot. Mol. Biol.*, F. M. Ausabel *et al.*, Eds. (Wiley, New York, 1989),

pp. 14.1.1–14.1.8]. Sections were hybridized with an <sup>35</sup>S-labeled antisense RNA probe made from a murine H19 complementary DNA (cDNA) [D. Sassoon and N. Rosenthal, in *Guide to Techniques in Mouse Development*, P. M. Wassarman and M. L. DePamphilis, Eds. (Academic Press, New York, 1993), pp. 384–404]. The slides were visualized with a Bio-Rad confocal microscope.

17. T. Tennenbaum *et al.*, *Cancer Res.* **52**, 2966 (1992).
18. We thank members of the Magnuson lab and B. Hogan for critical reading of the manuscript, C. Faust for help with confocal imaging, S. K. Dey, R. Schultz, D. L. Page, J. R. Goldenring, and D. Raiford for

helpful discussions, and K. Newsom for technical assistance. We are indebted to S. Wert and J. Whitsett (University of Cincinnati) for help with immunohistochemical analyses and interpretation of lung histology. D.W.T. was supported by NIH grants HD07104 and GM14630. This work was supported by NIH grants HD26722 (T.M.), NS18381 (K.H.), CA46413 (R.J.C.), DK39261 (R.C.H.), and P30DK26657 (J.A.B.). R.J.C. and R.C.H. are VA Clinical Investigators. R.J.C. acknowledges support by the Joseph and Mary Keller Foundation.

10 April 1995; accepted 31 May 1995

## Strain-Dependent Epithelial Defects in Mice Lacking the EGF Receptor

Maria Sibilia and Erwin F. Wagner

Mice and cells lacking the epidermal growth factor receptor (EGFR) were generated to examine its physiological role in vivo. Mutant fetuses are retarded in growth and die at mid-gestation in a 129/Sv genetic background, whereas in a 129/Sv  $\times$  C57BL/6 cross some survive until birth and even to postnatal day 20 in a 129/Sv  $\times$  C57BL/6  $\times$  MF1 background. Death in utero probably results from a defect in the spongiotrophoblast layer of the placenta. Newborn mutant mice have open eyes, rudimentary whiskers, immature lungs, and defects in the epidermis, correlating with the expression pattern of the EGFR as monitored by  $\beta$ -galactosidase activity. These defects are probably cell-autonomous because chimeric mice generated with EGFR<sup>-/-</sup> embryonic stem cells contribute small amounts of mutant cells to some organs. These results indicate that the EGFR regulates epithelial proliferation and differentiation and that the genetic background influences the resulting phenotype.

The EGFR (or *ERBB1*) belongs to a family of tyrosine kinase receptors (which includes *ERBB2/NEU*, *ERBB3*, and *ERBB4*) that show heterodimerization in vitro (1). Several ligands such as EGF, transforming growth factor- $\alpha$  (TGF- $\alpha$ ), heparin-bound EGF, betacellulin, and amphiregulin can bind the EGFR and regulate many cellular processes (1). During mouse development, the receptor can be detected on the trophoblast of the blastocyst and continues to be expressed together with several EGFR ligands in the placenta, uterus, and decidua (2–4). At mid-gestation, EGF binding activity can be detected in various organs, but only a few studies have localized the EGFR in specific tissues or cell types (4). In adult mice, the EGFR is expressed strongly in the liver and in tissues with regenerative epithelium, such as skin and gut (4). Amplification and overexpression of the EGFR has been detected in many human tumors of epithelial origin and in glioblastomas (4).

The gene encoding the EGFR was inactivated by replacement of part of the first exon with an *Escherichia coli lacZ* reporter gene. Single- (+/-) and double-targeted (-/-) embryonic stem (ES) clones were obtained at high frequency in two different

ES cell lines (5, 6) (Fig. 1A). EGFR<sup>-/-</sup> ES cells are viable and not impaired in their growth potential (7). Several chimeras transmitted the mutated allele to their offspring, and heterozygote mice of both sexes were healthy and fertile (8). When inbred 129 EGFR<sup>+/-</sup> mice were intercrossed, no live -/- offspring were found at embryonic day 12.5 (E12.5) (Table 1). Earlier in their development, mutant embryos were obtained at the expected Mendelian frequency, indicating that implantation and early post-implantation development were not impaired (Table 1). A reduction in the number of live homozygote mutants was observed after E11.5 on a 129  $\times$  BL6 background; however, a small number of mutant fetuses developed to term. In a 129  $\times$  BL6  $\times$  MF1 background, three mutant mice survived until postnatal day 20 (P20) (Table 1). The absence of EGFR mRNA and protein in mutant primary embryonic fibroblasts and E13.5 embryos was confirmed by Northern (RNA) and protein immunoblot analysis (Fig. 1, B and C).

Mutant embryos were slightly reduced in size and weight from E10.5 on a 129 background and from E13.5 on a mixed 129  $\times$  BL6 background (Fig. 2A) (7). The three 129  $\times$  BL6  $\times$  MF1 EGFR<sup>-/-</sup> mice, which survived until P20, were only 40 to 50% of the size and weight of control littermates (7). The reduced body weight of the EGFR<sup>-/-</sup>

fetuses was most likely a consequence of the smaller placentas (Fig. 2, A and B). E13.5 mutant placentas were structurally abnormal, and the maternal decidua was more easily separable by manual dissection from the fetal components. The spongiotrophoblast layer was reduced in size, with only a thin layer of *flt-1*- and 4311-expressing spongiotrophoblast cells (Fig. 2, C through E, and G) (7, 9). The labyrinthine trophoblast cells and the network of embryonic vessels and maternal sinuses appeared structurally normal (Fig. 2, C and D), as shown by the expression of *flk-1* in the endothelial cells of the labyrinth (Fig. 2, F and H) (10). Secondary giant cells were present in normal numbers and formed multiple cell layers at the interface between the maternal decidua and the embryonic labyrinth (7). Thus, the absence of the EGFR appears to specifically affect the proliferation or survival of spongiotrophoblast cells.

**Table 1.** Viability of offspring from EGFR heterozygote matings in three mouse strains. Genotype analysis of embryos (E9.5 to E18.5), newborn (P1), and adult (P20) offspring from EGFR heterozygote parents in three genetic backgrounds (8). After cesarean section, none of the live E18.5 EGFR<sup>-/-</sup> fetuses sustained respiration for longer than 1 hour, and all 129  $\times$  BL6 newborn fetuses (some with milk in their stomachs) died within 12 to 24 hours. Dead EGFR<sup>-/-</sup> embryos and mice are indicated in squared brackets. +/+, wild-type; +/-, heterozygotes; -/-, homozygote mutants.

Mouse strain	Offspring			Total (litters)
	+/+	+/-	-/-	
<i>E9.5 to 11.5</i>				
129	16	27	12	55 (8)
129 $\times$ BL6	31	69	26 [1]	127 (12)
<i>E12.5 to 13.5</i>				
129	26	42	0 [3]	71 (13)
129 $\times$ BL6	83	140	43 [8]	274 (37)
<i>E14.5 to 18.5</i>				
129	3	11	0	14 (3)
129 $\times$ BL6	94	157	17 [26]	294 (44)
<i>P1</i>				
129 $\times$ BL6	44	99	8 [5]	156 (19)
<i>P20</i>				
129; 129 $\times$ BL6	104	157	0	261 (31)
129 $\times$ BL6 $\times$ MF1	281	0 [3]	0	284 (30)

Research Institute of Molecular Pathology (IMP), Dr. Bohr-Gasse 7, A-1030 Vienna, Austria.